INL/JOU-15-35686
PREPRINT

Low-Potential Electrochemical Oxidation of 243Am(III) in Nitric Acid By a Derivatized, High Surface Area Metal Oxide Electrode

Dares, Christopher J.
Lapides, Alexander M.
Mincher, Bruce J.
Meyer, Thomas J.

November 2015

The INL is a
U.S. Department of Energy
National Laboratory
operated by
Battelle Energy Alliance

Low-Potential Electrochemical Oxidation of ^{243}Am(III) in Nitric Acid By a Derivatized, High Surface Area Metal Oxide Electrode

Christopher J. Dares,[a] Alexander M. Lapides,[a] Bruce J. Mincher,[b] Thomas J. Meyer*,[a]

a Department of Chemistry, The University of North Carolina at Chapel Hill, Chapel Hill, North Carolina 27599. b Idaho National Laboratory, Aqueous Separations and Radiochemistry Department, Idaho Falls, ID, USA

*e-mail: tjmeyer@unc.edu

A high surface area, tin-doped indium oxide electrode surface-derivatized with a terpyridine ligand has been applied to the oxidation of trivalent americium to Am(V) and Am(VI) in nitric acid. Potentials as low as 1.8 V vs. the saturated calomel electrode are used, 0.7 V lower than the 2.6 V potential for one-electron oxidation of Am(III) to Am(IV) in 1 M acid. This simple electrochemical procedure provides, for the first time, a method for accessing the higher oxidation states of Am in non-complexing media for developing the coordination chemistries of Am(V) and Am(VI) and, more importantly, for separation of americium from nuclear waste streams.

Nuclear energy continues to be an attractive large scale energy source due to its high power density without affecting the global climate (*1*). However, there are drawbacks to its expanded use including the management of used fuel and high-level waste (HLW) (*2, 3*). In particular, allowing the minor actinide, americium, to remain in the nuclear waste stream greatly limits the storage capacity of geologic repositories due to heat production, especially from ^{241}Am, which is a major constituent contributing to the long-term radiotoxicity of HLW. Closed nuclear fuel recycle schemes that improve uranium efficiency and minimize the volume of high level waste are under development in nuclear energy programs worldwide. In these schemes, Am must be separated from the lanthanides for transmutation as a fuel component, rather than being interred in a high level nuclear waste repository. Separation from the lanthanides is essential due to their high neutron cross-sections the lanthanides

cannot be incorporated into recycled fuel. Hence, there is a need for a high degree of separation of Am from the lanthanides (*4*).

Partitioning of Am from the lanthanides is arguably the most difficult separation in radiochemistry. The stable oxidation state of Am in aqueous, acidic solutions is Am(III). With its ionic radius comparable to the radii of the trivalent lanthanide ions, its coordination chemistry is similar, leaving few options for separation. One approach is the use of soft donor ligands which exploit a very slight preference for the more covalently bonded actinide 5f electrons over lanthanide 4f electrons. Notable progress has been made in complexation-based strategies but significant challenges have been encountered, stimulating efforts to find alternatives. Another approach is oxidation and separation using the higher oxidation states of Am (*5, 6*). Unlike the lanthanides, Am(III) can be oxidized to Am(V) and Am(VI), as $[Am^{V}O_2]^{+}$ and $[Am^{VI}O_2]^{2+}$, in acidic media. The high oxidation states have significantly altered charge densities and can be separated from the lanthanides by well-developed solvent extraction methods (*4*), and provides a platform for new extraction technologies.

Penneman and Asprey first reported the generation of Am(V) and Am(VI) in the 1950s (*7*). Determination of the formal redox potentials has relied on direct electrochemical measurements or by indirect measurements by calorimetry. Formal potentials for the Am(IV/III) couple were evaluated in the 1960s-1970s in concentrated phosphoric acid solutions (≈ 2-15 M) with Am(IV) stabilized by phosphate coordination, and Am(V) destabilized, decreasing the driving force for disproportionation (*8-12*). Am(IV) is also stabilized in mildly acidic, concentrated fluoride solutions (*13*). Values for the Am(IV/III) potential have fluctuated from as low as 2.2 V to as high as 2.9 V, with the standard value of 2.62 V vs. SCE in 1 M perchloric acid derived from enthalpy of formation measurements by Morss and Fuger (*14, 15*). The accepted $[AmO_2]^{2+}/[AmO_2]^{+}$ redox potential of 1.6 V vs. SCE in 1 M acid is based on direct electrochemical measurements by Penneman and Asprey (*7*). No electrochemical data are

available for the $[AmO_2]^+$/Am(III) couple and a value of 1.72 V vs. SCE in 1 M has been obtained based on calorimetric measurements.

Multiple challenges exist in oxidizing Am(III) to its higher oxidation states in non-complexing media, most notably the high potential for the intermediate Am(IV/III) couple (**Figure 1**) (*15*). Only a limited number of chemical oxidants, including persulfate, and bismuthate, have been explored for this purpose (*16*). Adnet and coworkers have patented a method for the electrochemical generation of high oxidation state Am in nitric acid solutions (*17*). Their method is based on earlier results by Milyukova *et al.* (*18, 19*) who demonstrated Am(III) oxidation to Am(VI) in acidic persulfate solutions with Ag(I) added as an electron transfer mediator with E^o(Ag(II/I)) = 1.98 V vs. SCE). In both measurements, phosphotungstate was added to coordinate Am with formation of a heteropolyanion complex facilitating electron transfer. However, separation schemes involving phosphotungstate failed due to interferences.

Electrochemical generation of Am(VI) in the absence of chemical additives opens new separations options with relatively simple process systems, while greatly minimizing secondary waste production and treatment. Chemical oxidation with persulfate as an oxidant, gives sulfate as a byproduct which prevents subsequent vitrification of the waste (*20*). Bismuthate suffers from very low solubility necessitating a filtration step which complicates its removal (*16*). Electrochemical oxidation combined with solvent extraction has the potential to contribute to a greatly simplified fuel cycle with a significant decrease in associated cost.

The coordination chemistry of Am(VI) is almost unknown because of the difficulties in its generation, its instability, and interferences caused by chemical oxidants or their byproducts. The inability to explore its coordination chemistry has led to a dearth of information about selective ligand affinities for Am(VI). Typically, assumptions about Am(VI) coordination chemistry are based on analogy

to the behavior of U(VI), which also exists as the dioxocation $[UO_2]^{2+}$ (*21*). An electrochemical method for generating the higher oxidation states of Am in non-complexing media without interferences from chemical oxidants and their reduction products could greatly facilitate advances in Am(VI) coordination chemistry.

The ability to generate Am(V) in the absence of additives also enables additional separation strategies. Due to its low charge density, the $[AmO_2]^{+}$ ion is not highly complexed and not extracted by ligands suitable for lanthanide separation leaving Am(V) in the raffinate. This approach has been investigated with bismuthate oxidation but, ultimately failed because the reduced Bi(III) product interfered with lanthanide extraction, a disadvantage that could also be overcome by electrochemical oxidation (*16*).

We have approached the oxidation challenge electrochemically by application of surface modified electrodes. The results described here provide the first demonstration that both Am(V) and Am(VI) can be generated electrochemically in nitric acid solutions at potentials well below the Am(IV/III) potential by exploiting modified electrode surfaces. They open up new avenues for fundamental studies and new approaches to nuclear waste processing.

We have pioneered the development and fabrication of high surface area porous oxide electrodes adapted for electrochemistry. They include planar fluoride-doped tin oxide (FTO) glass and reticulated vitreous carbon (RVC) coated with thin layers of conducting nanoparticle oxides; notably tin-doped indium oxide (ITO), antimony-doped tin oxide (ATO), and FTO (*22, 23*). These electrodes have multiple advantages including high conductivities, high surface areas, and well-developed chemistry for surface modification and derivatization (*22-24*).

Surface modification by covalent attachment of molecules can dramatically alter electrode behavior by imparting the reactivity and interfacial properties of the molecules to the surface. Examples

from our previous work have included electrocatalysis with surface-bound Ru(II) polypyridyl-based electrocatalysts, and assemblies (*25, 26*). The resulting modified electrodes carry out a variety of catalytic reactions including water oxidation and C-H functionalization (*26, 27*). In this extension to Am oxidation, we derivatized mesoscopic metal oxide nanoparticle electrodes with covalently attached 4'-phosphonyl-(4-phenyl)-2,2':6',2"-terpyridine p-tpy as a surface-bound ligand. As shown in Figure 2, it binds to the metal oxide through the phosphonic acid group creating a tpy-based surface binding site with an extensive and well-established d-block transition metal coordination chemistry, and the ability to coordinate Am(III). N-donor ligands were chosen because they have often been used for Am(III) separation in liquid-liquid extraction (*28, 29*). They are oxidatively robust in acidic solutions and have sufficient affinity for Am(III) to be useful in surface electrochemical oxidation (*28-30*). By using a p-tpy-modified, high surface area oxide electrode, we demonstrate here, for the first time, the electrochemical oxidation of Am(III) to Am(V) and Am(VI) in nitric acid solutions without the use of added ligands to the external solution. It is notable that these modified electrodes support oxidation of Am(III) at potentials as low as 1.8 V vs. SCE in 0.1 M acid, far below the 2.6 V vs. SCE potential for the one-electron couple in 1 M acid.

*Preparation and characterization of electrodes modified with p-tpy, nano*ITO-p-tpy. A 200 mg/mL suspension of sonicated *nano*ITO (particle size 20 – 50 nm) in ethanol (15 % acetic acid v/v) was spin-coated onto freshly cleaned FTO slides (15 Ω/cm) at 600 rpm. Thickness was measured by SEM to be approximately 8 μm. The electrodes were annealed in air at 450 °C for 1 h, and allowed to slowly cool to room temperature. They were then derivatized by immersion in a solution of 1 mM p-tpy in methanol, by soaking for at least 2 h, prior to use.

Cyclic voltammograms of non-derivatized, and derivatized electrodes feature differences in capacitance, and current at high anodic potentials (Figure S1). These are important effects with derivatization of *nano*ITO with p-tpy resulting in noticeably higher capacitive backgrounds and lower

anodic currents at potentials beyond the thermodynamic potential for water oxidation at 1.17 V vs. NHE at pH 1. Based on these results, derivatization of *nano*ITO with p-tpy increases the over-potential for water oxidation, in turn increasing the faradic efficiency for Am oxidation.

The surface coverage of p-tpy on *nano*ITO was estimated to be 4.1×10^{-9} mol·cm^{-2}; determined by placing a 0.6 cm^2 electrode in a 1mM solution of $Fe(ClO_4)_2$ for 20 min, and then measuring the charge passed through the $[Fe(p\text{-}tpy)]^{3+/2+}$ surface wave at 0.93 V vs. SCE in 0.1 M nitric acid by cyclic voltammetry (Figure S2). This value is a lower limit since it is based on surface formation of a $[Fe(p\text{-}tpy)_2]^{2+}$ couple and coordination of two p-tpy ligands. Surface analysis by monitoring the p-tpy-based ligand reduction wave for *nano*ITO-$[Fe(p\text{-}tpy)_2]^{2+}$ at ≈ -1 V was not possible because of interference due to reduction of Sn(II) sites on the electrode surface which occurs prior to ligand reduction.

Procedure for the spectroelectrochemical oxidation of Am(III). Two experimental protocols were employed for spectrophotometric monitoring of Am-containing solutions during the course of the electrochemical oxidations. In both, a two compartment cell with compartments separated by a fine glass frit was used for the electrochemical oxidation. A portion of the electrolyte was transferred either manually to a 1 cm quartz cuvette at various times, or, with continual flow by using a custom-controlled peristaltic pump connected to a World Precision Instruments 50 cm capillary waveguide for speciation measurements. An Ocean Optics HR4000 spectrometer was used to record absorbed light output from an Advanced Light Source DH-1000. When using the peristaltic pump in conjunction with the 50 cm waveguide, spectra were recorded at pre-determined time intervals. Speciation of Am was evaluated during electrolysis by measurement of the f-f transitions of Am(III) (504 nm, $\epsilon \approx 300$ L·mol^{-1}·cm^{-1}), Am(V) (718 nm, $\epsilon \approx 60$ L·mol^{-1}·cm^{-1}), and Am(VI) (666 nm, $\epsilon \approx 27$ L·mol^{-1}·cm^{-1}).

Electrochemical oxidation of Am(III). Controlled potential electrolyses were carried out at various potentials in 0.1 M nitric acid, with 0.9 M added sodium nitrate to retard migration of Am across the frit

to the counter electrode. Am concentrations varied, but were checked by γ-spectroscopy using 5 minute count times. Aliquots of the counter-electrode compartments at the end of the electrolysis periods were counted by γ-spectroscopy with the results confirming that Am migration across the frit had not occurred. No Am(III) oxidation was observed using un-derivatized electrodes at potentials between 1.8 and 2.7 V vs. SCE. Noticeable electrode decomposition was evident at potentials above 2 V for electrolysis periods as short as 1 h. Possible Am adsorption on both derivatized and un-derivatized ITO electrodes was investigated by mixing varying amounts of ITO powder into solutions of Am(III) at 1 μM. The ITO was filtered off, digested in 6.5 M nitric acid, and the resulting solution counted by γ-spectroscopy. No appreciable Am intercalation or adsorption into the ITO was observed in either case.

Spectroelectrochemical oxidation of Am(III). Visible absorption spectra of a solution containing 0.43 mM ^{243}Am(III) were acquired at regular time intervals during an electrolysis at 1.8 V in order to ascertain oxidation state speciation. At this potential and initial concentration, a decrease in Am(III) with time is observed with the concurrent ingrowth of Am(V) (Figure 3). The low molar extinction coefficients for the f-f transitions necessitated modeling the acquired spectra by a gaussian peak analysis. No Am(VI) was detected at this applied potential with mass balance reached by accounting for Am(III) and Am(V) in the solution. No changes in speciation were observed beyond 60 min, with approximately half of the Am(III) oxidized to Am(V) (0.19 mM Am(V), 0.25 mM Am(III)). At this potential, Am(VI) is accessible, and its absence is attributed to the slow electrochemical oxidation of Am(V) with competing auto-reduction of Am(VI) as it is formed. Increasing the total Am concentration to 0.95 mM, with initial Am(III) and Am(V) concentrations of 0.55 mM and 0.40 mM respectively (Figure S4), Am(V) is rapidly converted to Am(VI) at 1.8 V, while oxidation of Am(III) was slow. At pH 1 the potentials for the two couples are comparable, 1.60 V for Am(VI/V) and 1.61 V for Am(V/III), but rapid Am(VI/V) oxidation is consistent with simple electron transfer oxidation of $[AmO_2]^+$ to $[AmO_2]^{2+}$ while oxidation of aquated Am(III) to $[AmO_2]^+$ is more complex involving a change in coordination number and oxo formation.

The electrolysis results described here are significant, demonstrating for the first time, formation of high oxidation state Am, in this case, below the potential for the intermediate one-electron Am(IV/III) couple at 2.6 V in non-complexing media. The surface-bound p-tpy ligand is key to this "under-potential oxidation". Coordination of p-tpy to Am(III) at the electrode surface presumably decreases the thermodynamic barrier for the one-electron oxidation to Am(IV). Ligation effects are known to play an important role for Am(III). For example, formation of the 1:1 complex between Am(III) and 2-amino-4,6-di-(pyridine-2-yl)-1,3,5-triazine in a methanol-water mixture occurs with a $\Delta G° = -32.9$ kJ/mol (*28, 31*). By contrast, ligation effects for $[AmO_2]^+$ are expected to be negligible. Due to its instability, no information on the coordination preferences of Am(IV) towards N-donors exists, however, based on analogous studies of U(IV) and Pu(IV), Am(IV) is expected to remain bound and undergo electrochemical oxidation to Am(V) before diffusing from the electrode surface.

Scheme 1. Proposed mechanism for surface oxidation of Am(III) to Am(V) and Am(VI).

$$\text{Am(III)} + n\text{ITO|p-tpy} \rightleftharpoons n\text{ITO|p-tpy-Am(III)}$$

$$n\text{ITO|p-tpy-Am(III)} \xrightarrow{-e^-} n\text{ITO|p-tpy-Am(IV)}$$

$$n\text{ITO|p-tpy-Am(IV)} \xrightarrow{-e^-} n\text{ITO|p-tpy-Am(V)}$$

$$n\text{ITO|p-tpy-Am(V)} \xrightarrow{+2H_2O-4H^+} n\text{ITO|p-tpy} + [Am^{V}O_2]^+$$

$$[Am^{V}O_2]^+ \xrightarrow{-e^-} [Am^{VI}O_2]^{2+}$$

Reducing agents, including those generated radiolytically such as hydrogen peroxide are the culprits for the instability of Am(VI), and inhibit complete oxidation of Am(III). To demonstrate this, the applied potential and total Am concentration were varied, with spectroscopically monitoring.

Electrolysis of a 84 µM of Am(III) at 2.25 V, 130 mV below the Am(IV/III) couple, gives Am(V) and Am(VI), with both growing linearly with time (Figure 4). After one hour, the increase in Am(VI) remains linear but with a noticeable decrease in rate. The growth in Am(V) also slows after 1 h, eventually

levelling off to reach a steady state concentration of 30 μM. After 13 h of electrolysis, the composition of the solution was 9 μM (11 %) Am(III), 45 μM (54 %) Am(V) and 30 μM (36 %) Am(VI).

A further increase in applied potential to 2.7 V with 1.84 mM Am(III), sufficient to generate Am(IV) by direct oxidation at the electrode, resulted in an increase in the rate of appearance of Am(VI) relative to Am(V) without Am(V) reaching a steady state (Figure S5). After a 7 h electrolysis period, the solution composition was 0.14 mM (8 %) Am(III), 0.73 mM (40 %) as Am(V), and 0.97 mM (53 %) Am(VI), which represents the final highest proportion of Am(VI) generated electrochemically in these studies (Figure S6).

Auto-reduction kinetics. Auto-reduction by radiolytic intermediates provides an explanation for only partial oxidation of Am(III) to Am(V) and Am(VI) at the electrolysis steady state as observed here. Quantitating auto-reduction, and its role in defining the electrolysis steady state are important elements in possible electrochemical/separation schemes for Am. Compared to chemical oxidation, the electrochemical procedure offers the significant advantage of avoiding complications from oxidizing agents and their reduced forms (*16*).

Radiolysis of water by Am generates one-electron reducing agents such as H-atoms, and two electron reducing agents such as hydrogen peroxide, and other redox transients (*32*). The concentration of radiolysis products varies linearly with total Am concentration, with zeroth order reduction kinetics observed for the appearance or disappearance of Am species. Under these conditions, rate constants for these Am species during auto-reduction can therefore be derived from the slopes of concentration-time plots (*33, 34*).

Radiolytically produced one-electron and two-electron reductants provide independent pathways for Am(VI) reduction, with an overall rate constant for Am(VI) loss of 23.4×10^{-6} s^{-1} (Figure S7). The Am(IV) produced from the two-electron reduction of Am(VI) by radiolytic intermediate or

intermediates, presumable H_2O_2, rapidly disproportionates to Am(V) and Am(III). The reduction of Am(V) to Am(IV) or Am(III) is slow on this timescale (Figure S8). Therefore, the rate of appearance of Am(III) is due entirely to the disproportionation of Am(IV). The measured rate of Am(III) appearance is 7.3×10^{-6} s^{-1}, which infers that the rate of auto-reduction of Am(VI) to Am(IV) is 14.6×10^{-6} s^{-1}. The rate constant for the appearance of Am(V) was measured to be 16.4×10^{-6} s^{-1}, and is both due to the one-electron reduction of Am(VI), as well as the disproportionation of Am(IV). Subtracting the contribution from Am(IV) disproportionation (7.3×10^{-6} s^{-1}), the one-electron reduction rate to produce Am(V) from Am(VI) is 9.1×10^{-6} s^{-1}.

The proposed auto-reduction sequence is as follows:

$$Am(VI) \rightarrow Am(V): k = 9.1\times10^{-6}\ s^{-1}$$

$$Am(VI) \rightarrow Am(IV): k = 14.6\times10^{-6}\ s^{-1}$$

$$2Am(IV) \rightarrow Am(III) + Am(V): \text{fast}$$

$$Am(V) \rightarrow Am(III): \text{slow}$$

Conclusions. Our results demonstrate low-potential oxidation of Am(III) to Am(VI) in non-coordinating solutions at high surface area metal oxide electrodes derivatized with a surface-bound terpyridine ligand. The mechanism appears to involve surface binding of Am(III) and oxidation to Am(IV) followed by further oxidation to Am(V) with release as $[AmO_2]^+$. Electrochemical oxidation is in competition with auto-reduction by radiolysis intermediates with Am(VI) more susceptible to reduction than Am(V).

The ability of the electrochemical procedure to generate both Am(V) and Am(VI) opens a new door for the investigation of the coordination chemistry, and stability of these oxidation states. When integrated with established solvent extraction methods, it may provide a basis for the separation and partitioning of Am from nuclear waste streams.

References

1. D. J. Rose, *Science* **184**, 351-359 (1974).
2. A. S. Kubo, D. J. Rose, *Science* **182**, 1205-1211 (1973).
3. E. E. Angino, *Science* **198**, 885 (1977).
4. B. J. Mincher, L. R. Martin, N. C. Schmitt, *Solv. Extract. Ion Exch.* **30**, 445-456 (2012).
5. W. H. Runde, B. J. Mincher, *Chem. Rev.* **111**, 5723-5741 (2011).
6. B. J. Mincher *et al.*, *Solv. Extract. Ion Exch.* **32**, 153-166 (2014).
7. R. A. Penneman, L. B. Asprey, *Rep. AECU-936*, (1950).
8. Y. M. Kulyako, I. A. Lebedev, V. Y. Frenkel, T. I. Troimov, V. F. Myasoedov, *Radiokhimiya* **23**, 837-843 (1981).
9. I. A. Lebedev, *Radiokhimiya* **20**, 653-655 (1978).
10. I. A. Lebedev *et al.*, *Radiokhimiya* **18**, 652-658 (1976).
11. B. F. Myasoedov, V. M. Mikhailov, I. A. Lebedev, O. E. Koiro, V. Y. Frenkel, *Radiochem. Radioanal. Lett.* **14**, 17-24 (1973).
12. E. Yanir, M. Givon, Y. Marcus, *Inorg. Nuc. Chem. Lett.* **6**, 415-419 (1970).
13. E. Yanir, M. Givon, Y. Marcus, *Inorg. Nuc. Chem. Lett.* **5**, 369-372 (1969).
14. L. R. Morss, J. Fuger, *J. Inorg. Nuc. Chem.* **43**, 2059-2064 (1981).
15. A. J. Bard, R. Parsons, J. Jordan, *Standard Potentials in Aqueous Solution*. (Marcel Dekker, Inc., 1983).
16. B. J. Mincher, L. R. Martin, N. C. Schmitt, *Inorg. Chem.* **47**, 6984-6989 (2008).
17. J. M. Adnet, L. Donnet, P. Brossard, J. Bourges, U. S. P. Office, Ed. (United States of America, 1997), vol. 5609745.
18. M. N. Litvina, M. S. Milyukova, B. F. Myasoedov, *J. Radioanal. Nuc. Chem.* **121**, 355-363 (1988).
19. M. S. Milyukova, M. N. Litvina, B. F. Myasoedov, *Radiokhimiya* **25**, 706 (1983).
20. B. A. Moyer *et al.*, *Inorg. Chem.* **52**, 3473-3490 (2013).
21. T. S. Franczyk, K. R. Czerwinski, K. N. Raymond, *J. Am. Chem. Soc.* **114**, 8138-8146 (1992).
22. M. A. Méndez, C. J. Dares, L. Alibabaei, J. J. Concepcion, T. J. Meyer, U. S. P. P. Application, Ed. (2014).
23. M. A. Méndez, L. Alibabaei, J. J. Concepcion, T. J. Meyer, *ACS Cat.* **3**, 1850-1854 (2013).
24. Y. Tamaki, A. K. Vannucci, C. J. Dares, R. A. Binstead, T. J. Meyer, *J. Am. Chem. Soc.* **136**, 6854-6857 (2014).
25. P. Kang, Z. Chen, A. Nayak, S. Zhang, T. J. Meyer, *Energy Environ. Sci.* **7**, 4007-4012 (2014).
26. W. Song *et al.*, *J. Am. Chem. Soc.* **136**, 9773-9779 (2014).
27. M. K. Coggins, M. A. Mendez, J. J. Concepcion, R. A. Periana, T. J. Meyer, *J. Am. Chem. Soc.* **136**, 15845-15848 (2014).
28. M. Miguirditchian *et al.*, *Inorg. Chem.* **44**, 1404-1412 (2005).
29. P. Panak, J., A. Geist, *Chem. Rev.* **113**, 1199-1236 (2013).
30. A. Afsar, L. M. Harwood, M. J. Hudson, P. Distler, J. John, *Chem. Commun.* **50**, 15082-15085 (2014).
31. P. J. Panak, A. Geist, *Chem. Rev.* **113**, 1199-1236 (2013).
32. G. Choppin, J.-O. Liljienzin, J. Rydberg, C. Ekberg, *Radiochemistry & Nuclear Chemistry*. (Academic Press, ed. 4th, 2013).
33. A. A. Zaitsev, V. N. Kosyakov, A. G. Rykov, Y. P. Sobolev, G. N. Yakovlev, *Radiokhimiya* **2**, 348-350 (1960).

34. S. M. Woods, A. Cain, J. C. Sullivan, *J. Inorg. Nuc. Chem.* **36**, 2605-2607 (1974).

Acknowledgements

This research was supported by the US Department of Energy Office of Nuclear Energy, Fuel Cycle Research and Development Program, under DOE Idaho Operations Office contract DE-AC07-99ID13727. This research made use of equipment for electrode fabrication including homogenizer, spin-coater, and annealing furnaces funded by the UNC Energy Frontier Research Center: Center for Solar Fuels, supported by the U.S. Department of Energy Office of Science, Office of Basic Energy Sciences under award number DE-SC0001011. A.M.L. thanks the US Department of Defense, Air Force Office of Scientific Research, for funding through National Defense Science and Engineering Graduate Fellowship award FA9550-11-C-0028.

Author Contributions

C.J.D., T.J.M., and B.J.M. conceived experiments, A.M.L. synthesized the ligand p-tpy, C.J.D. prepared electrodes, designed and fabricated custom equipment, and conducted all experiments. C.J.D., T.J.M, and B.J.M. analyzed and interpreted data. C.J.D., A.M.L, B.J.M., and T.J.M. wrote the manuscript.

Additional Information

Supplementary information is available in the online version of the paper. Reprints and permissions information is available online at XX. Correspondence and requests for materials should be addressed to T.J.M.

Competing Financial Interests

The authors declare no competing financial interests.

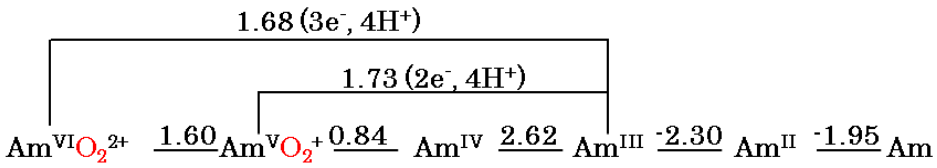

Figure 1 Latimer diagram for Am in 1 M perchloric acid. Potentials listed are vs. the saturated calomel electrode (SCE).

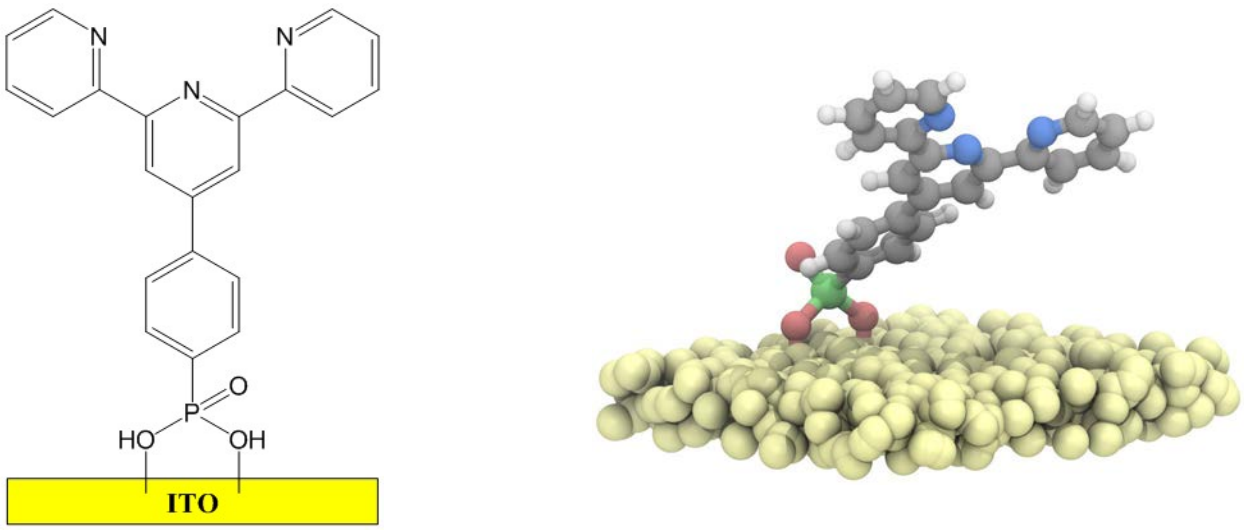

Figure 2. Molecular structure of p-tpy on the surface of an ITO particle. Protonation state is depicted as expected in neutral pH.

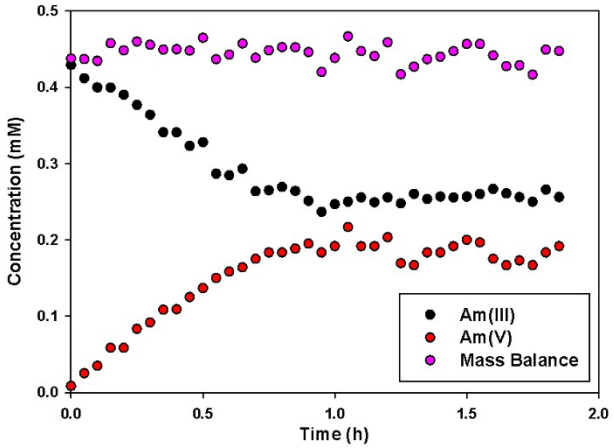

Figure 3. Am speciation measured by visible spectroscopy in a 1 cm cuvette at an applied potential of 1.8 V vs. SCE, showing the appearance of Am(V), concurrent loss of Am(III), and overall mass balance.

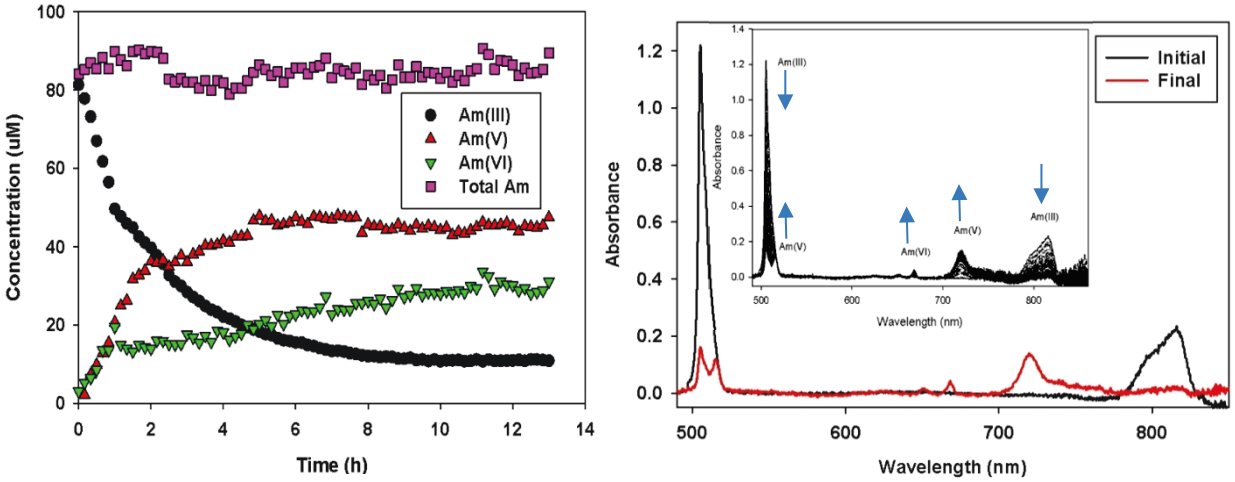

Figure 4. Am speciation as measured by visible spectroscopy in a 50 cm waveguide at an applied potential of 2.25 V vs. SCE.